

Characterization of a blue diode laser and diode laser driven by nanosecond pulses

Pawan Suthar

*A dissertation submitted for the partial fulfillment of
BS-MS dual degree in Science*

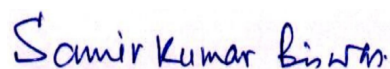


Department of Physical Sciences
Indian Institute of Science Education and Research
Mohali

April 2019

Certificate of Examination

This is to certify that the dissertation titled “**Characterization of a blue diode laser and diode laser driven by nanosecond pulses**” submitted by Pawan Suthar (Reg. No. MS14019) for the partial fulfillment of BS-MS dual degree programme of the institute, has been examined by the thesis committee. The committee finds the work done by the candidate satisfactory by the institute and recommends that the report be accepted.



Dr. Abhishek Chaudhuri

Dr. Samir K. Biswas

Dr. Kamal P. Singh
(Supervisor)

Dated: April 25, 2019

Declaration

The work presented in this dissertation has been carried out by me under guidance of Dr. Kamal P. Singh at the Indian Institute of Science Education and Research Mohali.

This work has not been submitted in part or in full for a degree, a diploma, or a fellowship to any other university or institute. Whenever contributions of others are involved, every effort is made to indicate this clearly, with due acknowledgement of collaborative research and discussions. This thesis is a bona-fide record of original work done by me and all sources listed within have detailed in the bibliography.

Pawan Suthar
(Candidate)

Dated: April 25, 2019

In my capacity as the supervisor of the candidate's project work, I certify that the above statements by the candidate are true to the best of my knowledge.

Dr. Kamal P. Singh
(Supervisor)

Acknowledgements

First and foremost, I would like to thank my project supervisor Dr. Kamal P. Singh for giving me the opportunity to work in his lab, suggesting ideas and projects to work on, and constant support throughout my stay at IISER Mohali. I would also like to acknowledge the guidance and help provided by Dr. Mehra S Sidhu. I also wish to thank the members of the Femtosecond Laser Lab for providing constant help and a stimulating environment during my time at the lab. A special note of thanks goes to Sanjay Kapoor for all his help and discussions during this thesis.

I would also like to thank my friends Anjani, Dharma, Jagmeet, Raman, Rishabh, Shivam, Vasudev, Virinder, and Vishal for making my time at IISER Mohali a lot more enjoyable. I would also like to thank my family members for their love.

List of Figures

1.1	Design of the laser diode mount.	3
1.2	Aluminium (Left) and Copper (Right) Heat Sink	4
1.3	For Heat Sink with base area 70 X 70 mm ²	4
1.4	Voltage and Output power as a function of current	5
1.5	Wavelength Spectra of the diode laser at different currents	6
1.6	Peak Wavelength as a function of temperature at 1.5A	6
1.7	Optical power as a function of temperature at 1.5A Current	7
1.8	Stability vs Current	8
1.9	Caption	9
1.10	Beam profile at 30 cm from the laser. The length unit is μm	9
1.11	Spot size as a function of distance near the waist. The data is fitted to find the beam waist position and	10
1.12	This shows the collimation of diode beam in the slow axis.	11
1.13	Focusing the beam in the crystal after collimation. The second image shows the spot size of the beam at the position of crystal.	12
2.1	Avalanche pulse generator based on Jim Williams. Source: [1]	16
2.2	electrical pulse generated from the transistor (a) 2N2369 and (b) 2N5192	17
2.3	Schematic diagram showing the dependence of carriers and photons in the cavity as a function of current.	18
2.4	Current, number of carriers and number of photons as a function of time.	21
2.5	Optical pulses as measured using a photodiode and oscilloscope.	22
A.1	Schematic diagram for the X-folded Ti:Sapphire laser cavity with two arms.	23
A.2	Spot size as a function of the cavity parameter δ	26

List of Tables

1.1	Dimensions of the mount, heat sink and TEC.	3
1.2	Area of the base vs. the maximum temperature reached	4
1.3	Stability of the laser diode optical power as a function of the current	7
1.4	Demonstration of direct diode pumped lasers over the year Adapted from [2]	13
A.1	ABCD matrices for various components of the oscillator	24

Contents

Certificate of Examination	iii
Declaration	v
Acknowledgements	vii
List of Figures	ix
List of Tables	xi
Abstract	xv
1 Blue diode laser	1
1.1 Diode mount and heating simulations	1
1.1.1 Choice of material: copper or aluminium	2
1.1.2 Dimension of the heat sink	3
1.2 Laser diode properties	5
1.2.1 Current, voltage, optical power and wavelength	5
1.2.2 Effects of temperature on the laser diode performance	5
1.2.3 Optical power stability	7
1.2.4 Spot size as a function of current	8
1.2.5 Finding the beam quality factor of the diode laser beam	8
1.3 Simulation of the beam shaping	10
1.4 Demonstrations of direct diode pumped Ti:S lasers	11
2 Semiconductor laser driven by nanosecond electrical pulses	15
2.1 Avalanche pulse generator	15
2.2 Nanosecond pulses generated from different transistors	16
2.3 Gain switching theory and simulations	18
2.4 Optical pulses from a laser diode	20

A	Finding the spot size in continuous case in a laser cavity	23
B	Beam shaping simulations	31
B.1	Before collimation	31
B.2	After collimation	35
C	Gain switching using RK4	39
	Bibliography	43

Abstract

We characterize a blue diode laser operating at a wavelength of approximately 470 nm and with an output optical power of 3.5 Watts. A laser diode mount cooled by thermo-electric cooler was designed and its performance was simulated in COMSOL. Beam shaping simulations of the diode laser beam were done to make it suitable for pumping a Ti:Sapphire laser.

A nanosecond electrical pulse generator using a transistor in avalanche mode was made and we obtained high amplitude nanosecond pulses. These electrical pulses were used to drive a semiconductor diode laser and 7 nanosecond optical pulses were obtained. We also show the dependence of the pulse duration on the current amplitude for gain switching via simulations.

Chapter 1

Blue diode laser

Nitride based semiconductors have a band gap between 2-6 eV which can produce light in a wide wavelength range from red to ultraviolet. Blue laser light has numerous applications in Blu-Ray DVD, white light generation, displays and projectors[3]. One interesting application of blue laser diode is to pump Ti:Sapphire laser[4]. Nakamura, Akasaki and Amano were awarded Nobel prize for their contribution to development of blue LEDs and diode lasers.

We have acquired a diode laser with rated output optical power of 3.5 Watts and wavelength around 470 ± 5 nm for the purpose of pumping a Ti:Sapphire laser. The rated driving current is 3.5 Amperes. We first design a diode laser mount to cool the laser diode and simulate its performance in COMSOL. We then thoroughly characterize the diode laser. We also perform beam shaping simulations to make the beam suitable for pumping a Ti:Sapphire laser.

1.1 Diode mount and heating simulations

The available laser diode mount in the lab (Thorlabs - TCLDM9) can cool a laser diode operated at a maximum current of 2A only. Since, the blue laser diode to pump the Ti:Sapphire laser is to be operated at a current of at least 3.5A, a custom made laser diode mount has to be made. The initial design of the mount and heat sink are made in SolidWorks 3D. To see if the designs can cool the laser diode, we simulated the cooling of the laser diode mount and heat sink in COMSOL simulation software.

The design consists of 3 separate components: the laser diode casing, two TECs and two heat sinks. The laser diode mount is designed to keep the temperature gradient across the mount to a minimum so as to allow stable operation of the laser diode. Therefore two TECs are used instead of one. The design of the laser diode is shown in Figure 1.1. The TECs are placed on two sides of the mount. Then heat sinks are in contact with hot side of the TEC, to help dissipate heat efficiently. Standard M4 and M3 screw holes are made at appropriate positions to secure the mount on the optical table and also to hold the three components (casing, TECs and heat sinks) in place. The dimensions of the various components are listed in Table 1.1.

To simulate the performance of the diode mount, we use the heat transfer module in COMSOL. We assume that the sides of the mount which are in contact with the TEC are kept at a constant temperature. We then assume that the diode laser casing acts as a uniform source of heat across the inner cylindrical boundary of the diode mount. The mount also dissipates heat to the environment via all the sides which are in contact with air. We fix the environment temperature to be 25°C . We assume no active cooling such as air or liquid cooling. The convective heat transfer coefficient is assumed to be $10\text{ W}/\text{m}^2\text{K}$.

To simulate the performance of the heat sink, we assume that the part of the heat sink in contact with the TEC acts as a boundary heat source. The heat sink will also lose heat to the environment by dissipation. We assume active cooling with air. The convective heat transfer coefficient is assumed to be $10\text{ W}/\text{m}^2\text{K}$.

The amount of heat dissipated by the heat sink should be the sum of heat dispersed from the cold side and the heat generated by the TEC. The heat to be dispersed from the cold side should be equal to the heat generated by the laser diode. A crude estimation will be $4\text{A} \times 5\text{Volts} = 20\text{ Watts}$ when output optical power from the laser diode is approximately 3.0 Watts . The heat generated by TEC is approximately 2.5 times the heat it disperses. Therefore total heat to be dissipated by the heat sinks should be around 70 Watts .

1.1.1 Choice of material: copper or aluminium

We simulated the performance of the mount made by two materials, Aluminium and Copper. The results are shown in Figure 1.2. The maximum temperature reached in

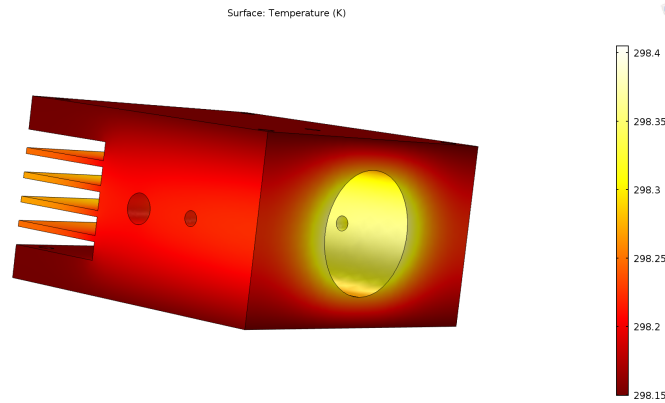


FIGURE 1.1: Design of the laser diode mount.

Dimensions of the Diode Casing	
Dimensions	70 X 70 X 30 mm ³
Cylindrical hole diameter	20.20mm
Dimensions of the Heat Sink	
Base	70 X 70 mm ²
Base Thickness	3.5 mm
Fin height	35 mm
Fin spacing	3 mm
Fin Thickness	1 mm
Dimensions of the TEC	
Base	40 X 40 mm ²
Thickness	3.9 mm

TABLE 1.1: Dimensions of the mount, heat sink and TEC.

case of Aluminium is 82°C and the temperature difference between the coldest and hottest parts of the sink is around 9°C. But for copper, the maximum temperature reached is 79°C and the temperature difference between the coldest and hottest parts of the sink is around 5°C. Therefore it is clear that we should use copper for better cooling of the laser diode, since price and weight of the material are not a major concern.

1.1.2 Dimension of the heat sink

To make the laser mount design to be future proof, since more and more powerful InGaN laser diodes are being made available, we need a mount that is able to cool even higher power laser diodes. To ensure that, I assumed that the heat dissipated by the

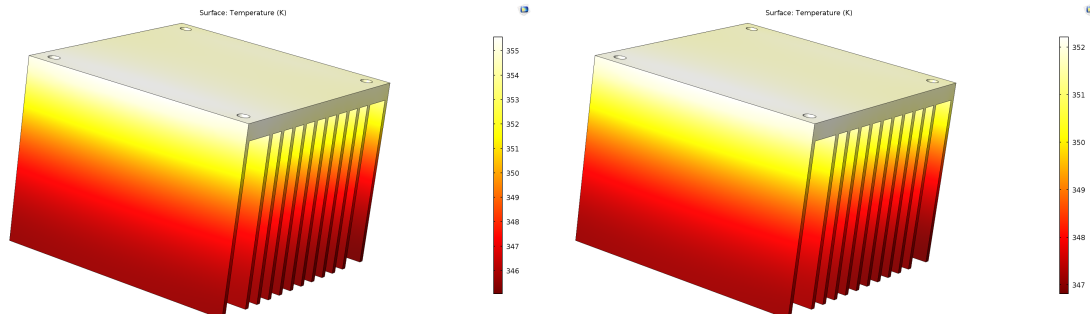
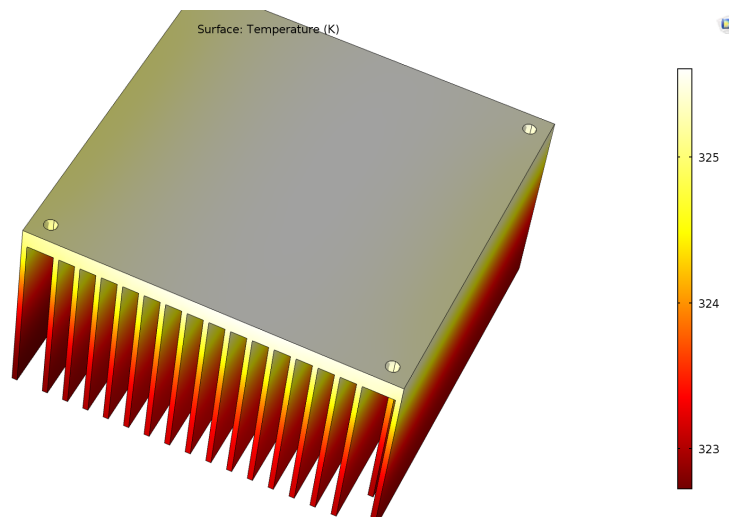


FIGURE 1.2: Aluminium (Left) and Copper (Right) Heat Sink

laser diode mount is 40 Watts, double of the previous estimate of 20 Watts for the laser diode at hand. If the efficiency of both laser diodes is similar, this would correspond to approximately 7 Watts of optical power. The total heat generated should be around 140 Watts including the heat generated by the two TECs. Therefore, we would have to use heat sinks that can dissipate atleast 70 Watts of heat while keeping the maximum temperature close to 50°C . The results are shown in Table 1.2. It is clear that for efficiently cooling the laser diode, the heat sink must have a base area of around $70 \times 70 \text{ mm}^2$.

Area of the Base	Max. Temp. ($^{\circ}\text{C}$)
$52 \times 52 \text{ mm}^2$	79
$60 \times 60 \text{ mm}^2$	64
$70 \times 70 \text{ mm}^2$	53

TABLE 1.2: Area of the base vs. the maximum temperature reached

FIGURE 1.3: For Heat Sink with base area $70 \times 70 \text{ mm}^2$

1.2 Laser diode properties

1.2.1 Current, voltage, optical power and wavelength

The electrical and optical characteristics of the laser diode are plotted in Figure 1.4. Wavelength of the diode laser was also measured using a spectrometer as a function of the laser diode current. Temperature was fixed at 25°Celsius. Wavelength spectra as a function of current are shown in the Figure 1.5.

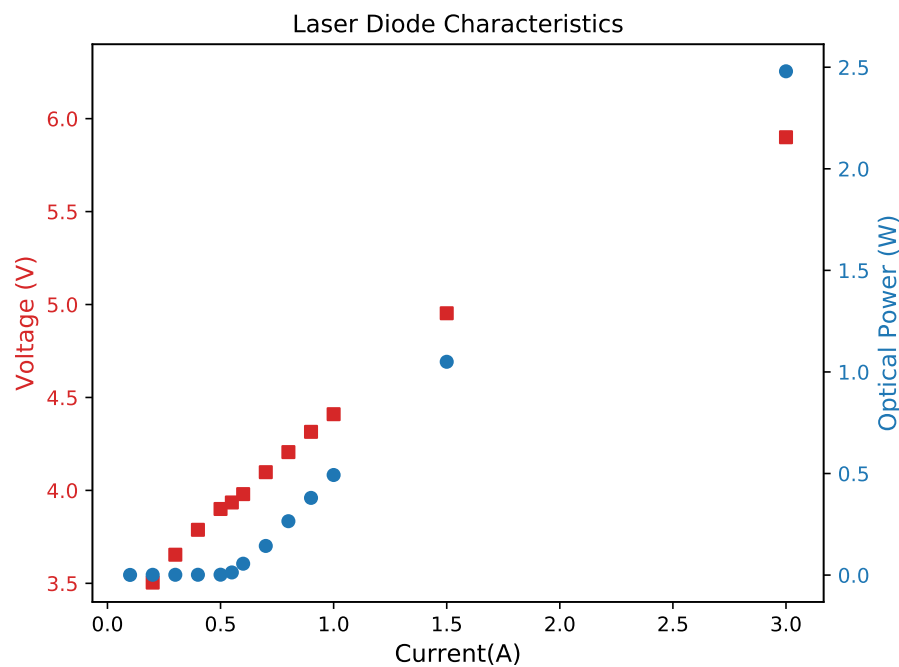


FIGURE 1.4: Voltage and Output power as a function of current

1.2.2 Effects of temperature on the laser diode performance

The wavelength of the laser diode may change due to change in temperatures[5]. Since, the laser has to be used for pumping Ti-Sapphire laser, where small change in wavelength may lead to a large change in absorption, therefore the wavelength of the laser diode is a very important parameter. Therefore we measured the wavelength of the laser diode at different temperatures. This is done by driving the laser diode at a constant current without any active cooling. The temperature of the diode will

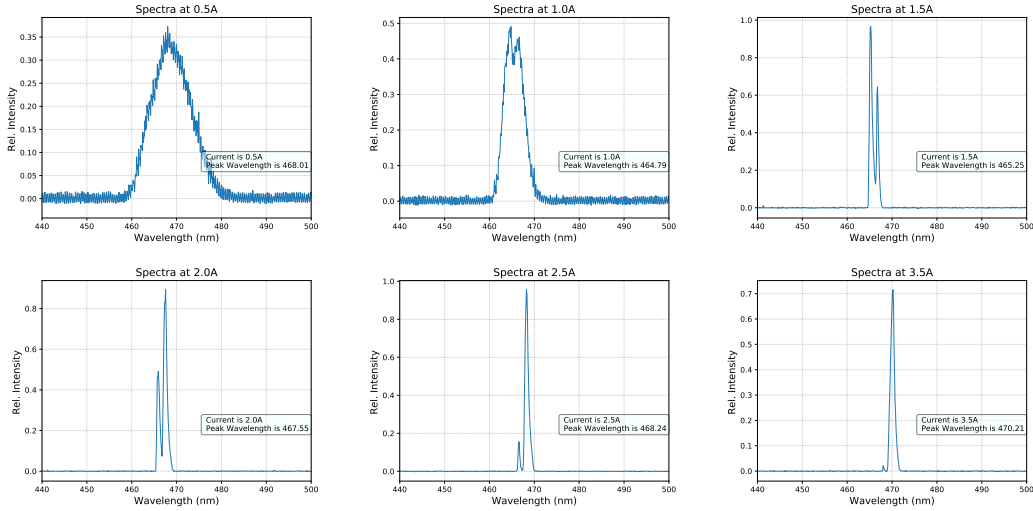


FIGURE 1.5: Wavelength Spectra of the diode laser at different currents

increase due to the heat produced. The results are shown in Figure 1.6. The results show that the change in wavelength is minimal and it will not significantly affect the pumping of Ti:Sapphire.

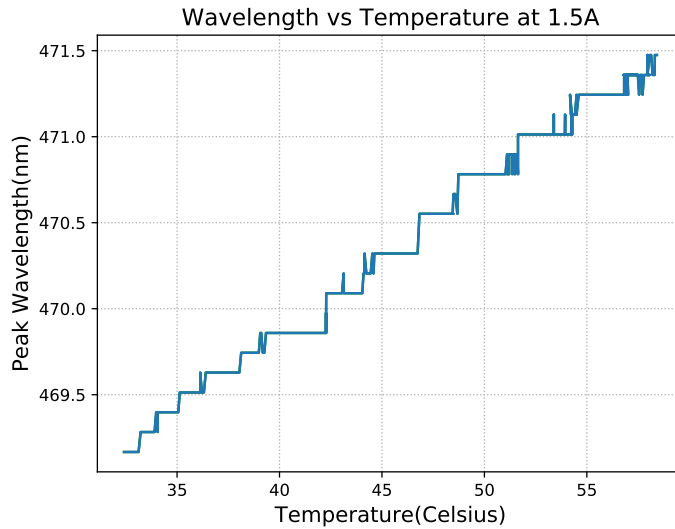


FIGURE 1.6: Peak Wavelength as a function of temperature at 1.5A

The optical power also changes with the temperature of the laser diode. To find the optimum temperature to operate the laser diode, we measured the optical power output as a function of the temperature of laser diode casing. The resulting plot of temperature vs the optical power is shown in Figure 1.7. It is clear that the diode

laser should be operated at a temperature as low as possible because the optical power decreases considerably with rising temperature.

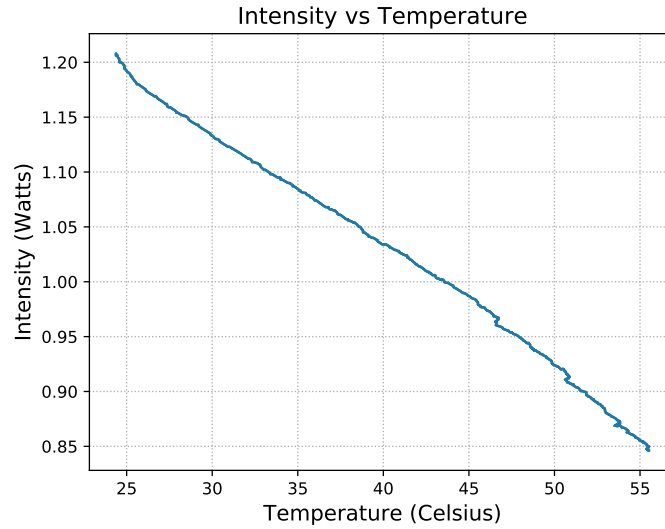


FIGURE 1.7: Optical power as a function of temperature at 1.5A Current

1.2.3 Optical power stability

Output power stability was measured using a photodiode and an oscilloscope. The results are shown in the Table 1.3 and the Figure 1.8 for various values of laser diode current. Here, Standard Deviation(%) is used which is $S.D.(%) = \frac{S.D.}{Mean} * 100$. Another parameter used to quantify is the Degradation which is defined as Average Power in the first 20 seconds minus the average power in the last 20 seconds of the measurement. Degradation(%) is then simply $\frac{Degradation}{Mean} * 100$. Negative values indicate that the power increased towards the latter part of the measurement.

Current (A)	S.D.(%)	Degradation(%)
1.5	0.39	0.51
2.0	0.59	1.0
2.5	0.42	-0.53
3.0	0.86	-2.92

TABLE 1.3: Stability of the laser diode optical power as a function of the current

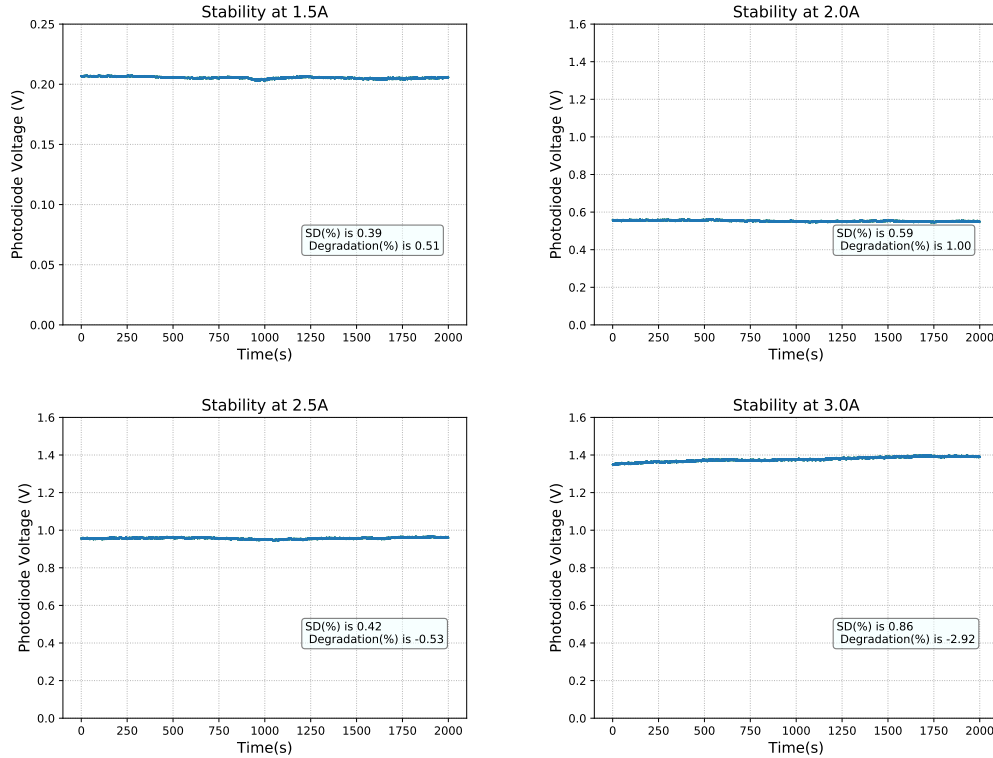


FIGURE 1.8: Stability vs Current

1.2.4 Spot size as a function of current

We fixed the distance between the Beam Profiler and the laser diode to approximately 30 cm and measured the beam diameter in x and y axis. The results are shown in Figure 1.9. We also show the beam profile in Figure 1.10. The beam spot size reduces with increasing the current. However at around 1.5A, the spot size increases. This may be due to effects of lasing threshold.

1.2.5 Finding the beam quality factor of the diode laser beam

M^2 factor is a measure of the laser beam quality. A perfect gaussian beam has a M^2 of 1 and it increases with decreasing beam quality.

$$\omega(z) = \omega_0 \left(1 + \left(\frac{M^2 \lambda z}{\pi \omega_0^2} \right)^2 \right)^{1/2} \quad (1.1)$$

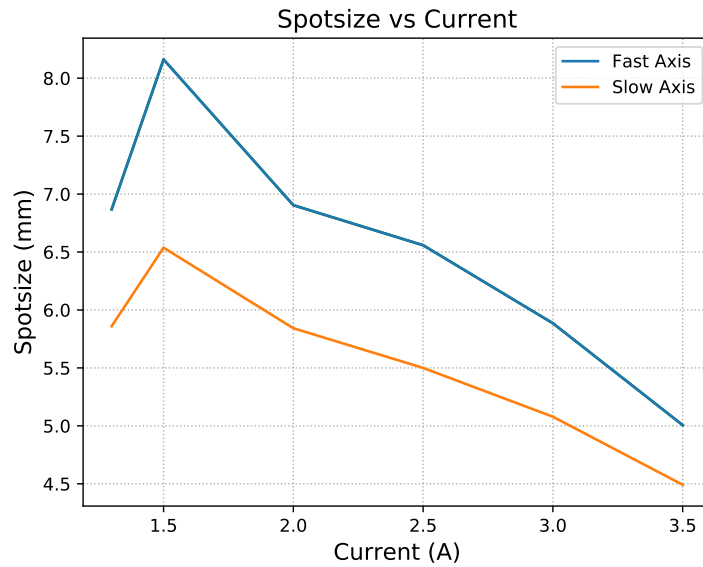
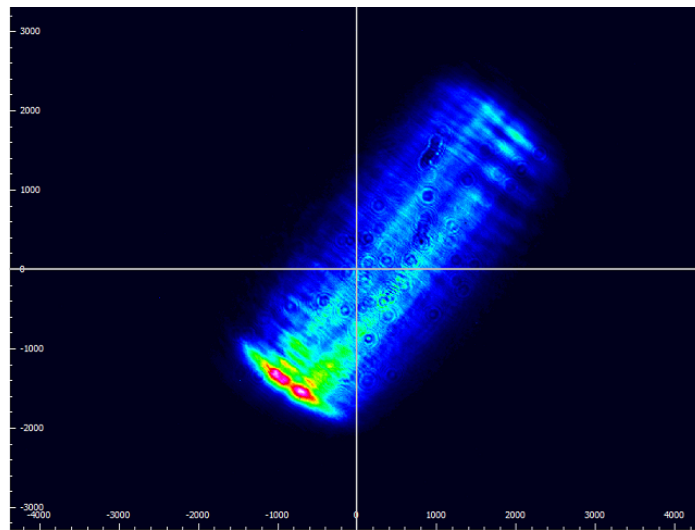


FIGURE 1.9: Caption

FIGURE 1.10: Beam profile at 30 cm from the laser. The length unit is μm

where z is the distance from beam waist and ω_0 is the beam spot size. We find the M^2 value by focusing the beam with a lens and measuring the spot size as a function of distance from a fixed point near the beam waist. Then we fit the spot size vs distance curve to obtain the M^2 value and beam waist position with Equation 1.1. The beam quality of the laser diode was measured to be 1.65 in the fast axis and 8.53 in the slow axis as shown in the Figure 1.11. This means that the beam will spread more in the slow axis if we focus them to the same spot size. This makes it harder to pump the Ti:Sapphire laser efficiently as discussed in the next section.

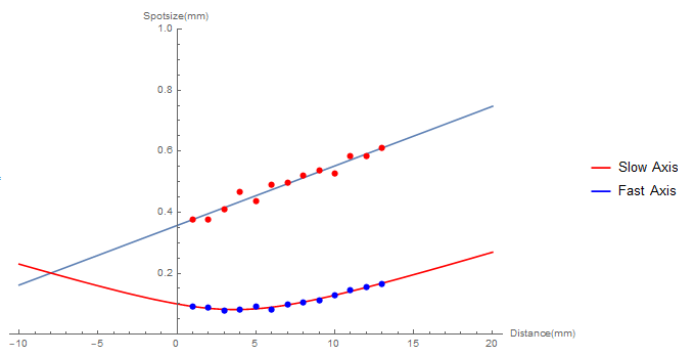


FIGURE 1.11: Spot size as a function of distance near the waist. The data is fitted to find the beam waist position and

1.3 Simulation of the beam shaping

We use ABCD matrices to simulate the beam profile of the diode laser beam as it propagates through various optical elements. The main goal of the beam shaping is to make the beam suitable for pumping a Ti:Sapphire crystal. A suitable beam will have a large spatial overlap with the laser mode. This means that the spot sizes and beam waist of the pump and laser mode should be similar in the crystal. Furthermore, the diode laser beam should have similar Rayleigh range (z_R) in the fast and slow axis. This is difficult due to the large difference in the M^2 values of the beam in the fast ($M^2=1.65$) and slow axis ($M^2=9$). Rayleigh range dependence on M^2 is given by,

$$z_R = \frac{\pi\omega_0^2}{M^2\lambda} \quad (1.2)$$

Therefore, we must find an appropriate beam shaping scheme for efficient pumping. [6] does it by using cylindrical lenses to have a good overlap between the pump and laser modes. We first collimate the fast axis using an aspheric lens. Then we find the beam diameter in the fast axis and the beam divergence and waist position (effectively q-parameter). Then we used this data and information from ref1 to model the beam shaping of the laser beam. To collimate the slow axis, ref1 first use a -50mm cylindrical lens to expand the slow axis to 5 times the fast axis. Then ref1 collimate the slow axis using a 500mm cylindrical lens as shown in Figure 1.12. The beam is now collimated. The beam is now focused in the crystal using a 105mm Lens. The beam finally passes through the dichroic cavity mirror with 100mm Radius of Curvature and is focused in the crystal as shown in Figure 1.13. From the beam shaping simulation we find a focal spot size at the crystal of $57 \times 100 \mu\text{m}$ which is similar to ref1.

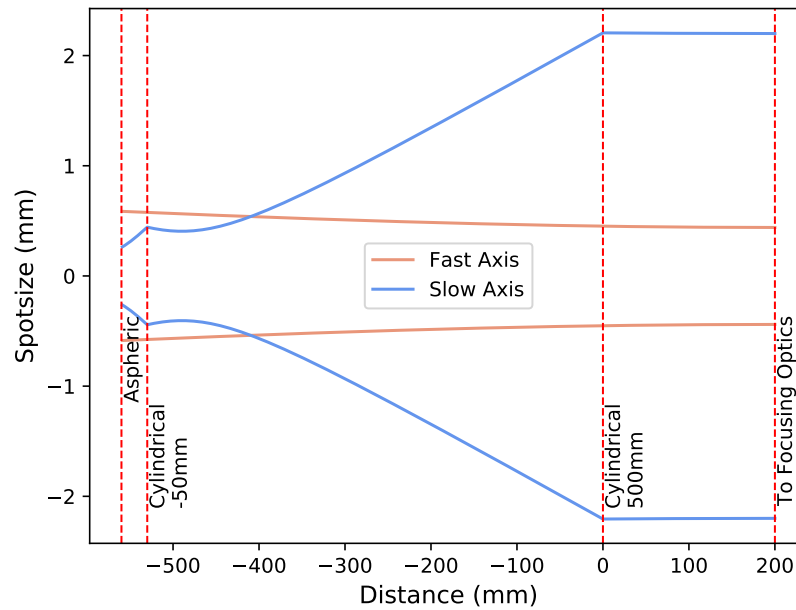


FIGURE 1.12: This shows the collimation of diode beam in the slow axis.

1.4 Demonstrations of direct diode pumped Ti:S lasers

As mentioned before, one interesting application of Nitride diode laser is to pump a Ti:Sapphire laser. The Table 1.4 shows the time line of developments in direct diode pumped Ti:Sapphire lasers. Roth, Kemp et al first demonstrated direct diode pumping of Ti:Sapphire laser in continuous mode in 2009[4]. Roth et al. also demonstrated first femtosecond direct diode pumped Ti:Sapphire laser by using SESAM mode-locking to achieve 114fs pulse duration[7]. In 2017, Backus et al. produced 14fs pulses from Ti:Sapphire oscillator pumped by a single 465nm blue laser diode similar to the one studied here[6].

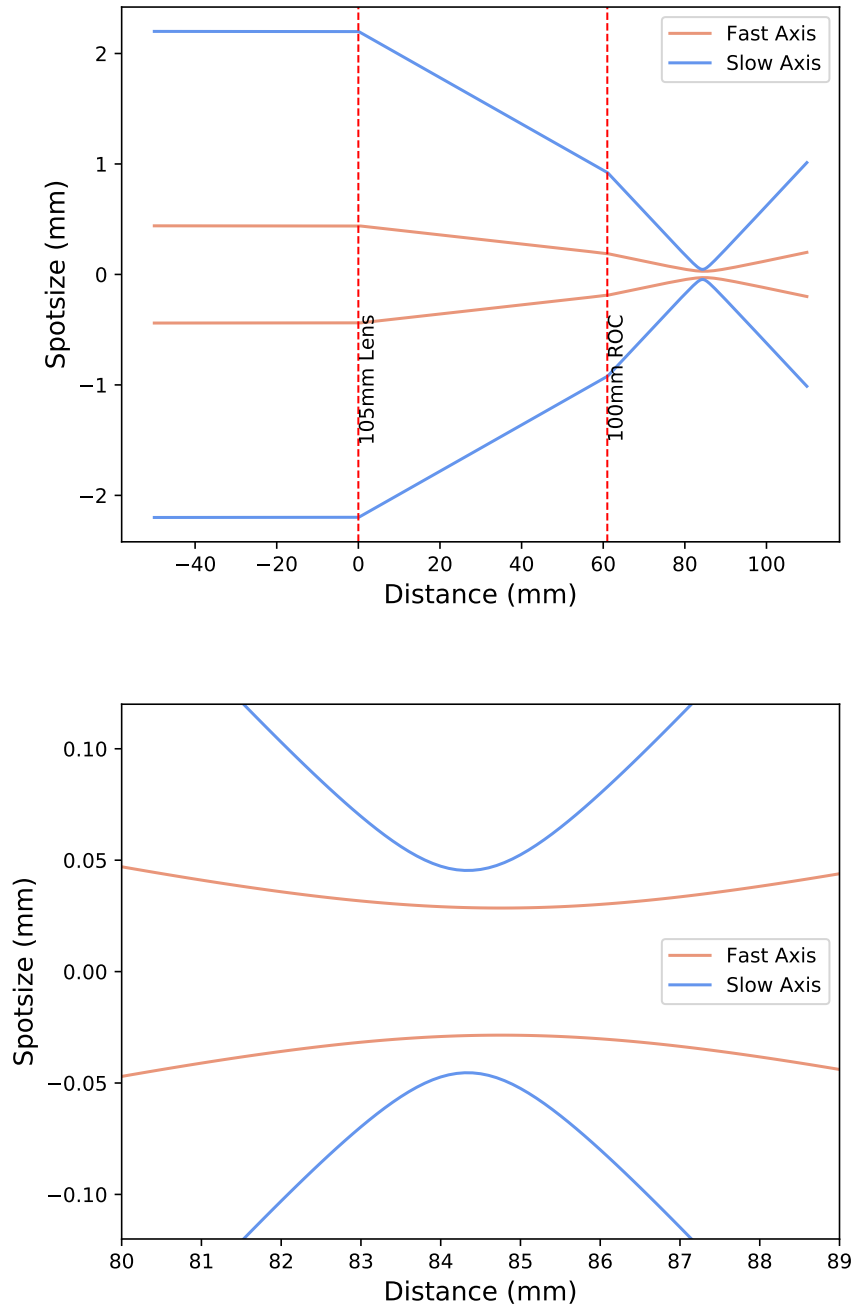


FIGURE 1.13: Focusing the beam in the crystal after collimation. The second image shows the spot size of the beam at the position of crystal.

Year	Author	Pump		Comments	Output	
		Wavelength	Power		Duration	Power
2009	Roth et al.[4]	452	1W	Continuous		19mW
2011	Roth et al.[7]	452	1W	SESAM Modelocked	114fs	13mW
2012	Durfee et al.[8]	445	2X1W	Kerr Lens Modelocked	15fs	34mW
2015	Tanaka et al.[9]	520	2X1W	Green Diode Pumping	74fs	45mW
2015	Gurel et al.[2]	520	2X1.5W	High Efficiency	39fs	450mW
2017	Backus et al.[10]	450	50W	Regenerative Amplifier	30fs	1W
2017	Backus et al.[6]	465	3W	Also wavelength multiplexing	14fs	173mW

TABLE 1.4: Demonstration of direct diode pumped lasers over the year
Adapted from [2]

Chapter 2

Semiconductor laser driven by nanosecond electrical pulses

Gain switching is a phenomenon where we can obtain picosecond pulses from semiconductor diode lasers if we pump them with high amplitude short current pulses [11]. The output optical pulses can be shorter than the input current pulses. The current pulses in our setup are generated from a high voltage avalanche pulse generator which produces high amplitude nanosecond current pulses. These pulses are then used to drive semiconductor diode lasers. This setup is very cost effective and the repetition rate of the output is tunable. Also we can swap out the diode lasers for different frequency diode lasers. This makes the setup very versatile.

2.1 Avalanche pulse generator

The schematic of the avalanche pulse generator is shown in the Figure 2.1. A high DC voltage is applied to the Collector junction via a resistor. The capacitor charges via the resistor and when the voltage reaches above the avalanche threshold for the transistor, the capacitor is discharged via the resistor connected at the emitter junction. The current pulse amplitude is decided by the transistor and the charge stored in the capacitor. The capacitor along with the output resistor also places a limit on the duration of the pulse.

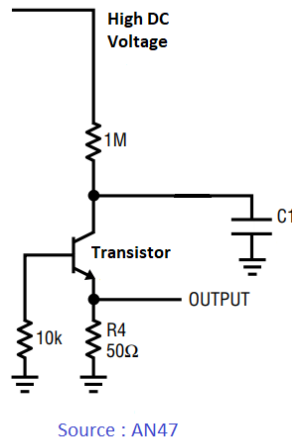


FIGURE 2.1: Avalanche pulse generator based on Jim Williams. Source: [1]

The output repetition rate depends on the C1 and high resistance connected to the high voltage. Also, it increases with increasing the high voltage because the capacitor reaches the avalanche breakdown voltage earlier. The repetition rate is limited by the heat dissipating capacity of the transistor. At high repetition rates, it may happen that the transistor is not able to dissipate the heat generated from one pulse before the next pulse arrives, this will lead to cumulative heating which will eventually break down the transistor.

2.2 Nanosecond pulses generated from different transistors

We tried different transistors to generate the electrical pulses. In the original paper [1], 2N2369 was used. But as evident from Figure 2.2 (a), the peak current of the electrical pulse is only 0.15 Amperes across 56 Ω . To drive semiconductor diode lasers and to generate short pulses, we would require very high peak currents. The need for high peak current electrical pulses is demonstrated in Figure 2.4.

Therefore, to achieve higher peak currents, we used transistor 2N5192. 2N5192 has avalanche breakdown at around 230 Volts compared to 60 Volts for the 2N2369. This is a power transistor and is therefore able to sustain higher currents. 2N5192 was also demonstrated to generate very high peak current pulses in avalanche mode in [12].

The electrical pulses generated from 2N5192 are shown in Figure 2.2 (b). These pulses have peak current of 5.45 Ampere across 56Ω which is almost 40 times higher than peak current from 2N2369. The pulse width is also very short at $\approx 7\text{ns}$ and therefore these pulses are ideal to drive a diode laser. The oscillations in the pulse are due to the lead inductance and capacitance.

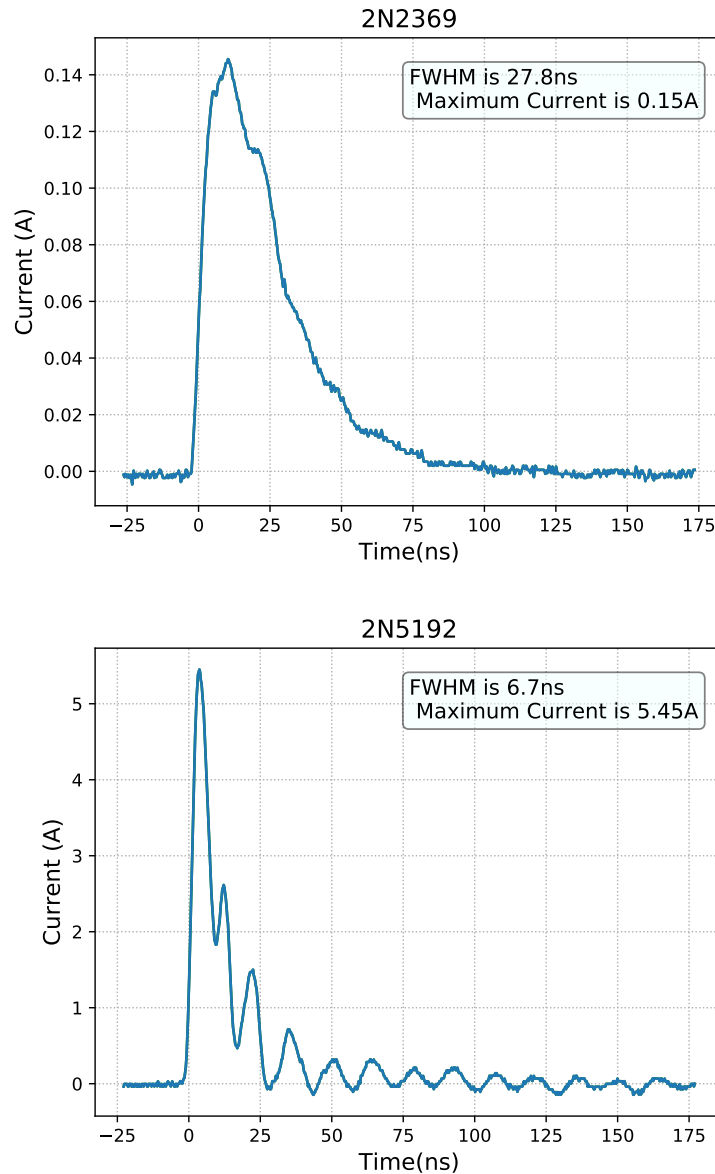


FIGURE 2.2: electrical pulse generated from the transistor (a) 2N2369 and (b) 2N5192

2.3 Gain switching theory and simulations

Gain switching is a technique where we vary the optical gain of the laser to produce extremely short pulses of the order of picosecond. In continuous operation the number of carriers in the excited state are equal to the threshold and if we increase the current further only the number of photons in the cavity increases and not the number of electrons. We plot the number of carriers in the excited state and the number of photons in the cavity vs the input current below in the continuous case (calculated from the equations described below). If we increase the current provided to the laser

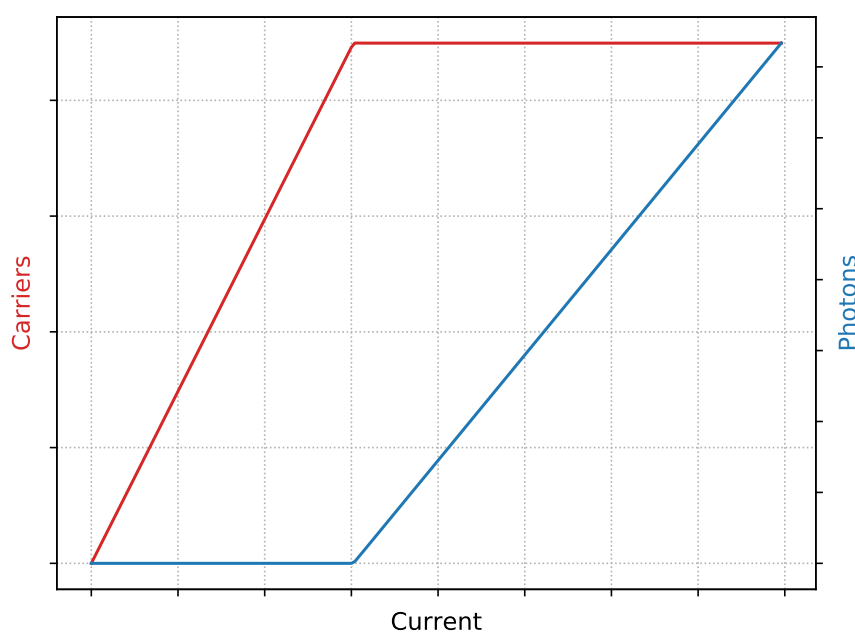


FIGURE 2.3: Schematic diagram showing the dependence of carriers and photons in the cavity as a function of current.

suddenly, the number of the carriers (electrons) in the laser cavity in the excited state will rise above the threshold. The number of carriers increase above the threshold for only a short time before coming below the threshold due to stimulated emission, giving rise to a short optical pulse. This is the phenomenon of gain switching. With suitable current pulses, we can obtain picosecond optical pulses. The lower limit on the pulse duration is set by the cavity round trip time.

To model the effects of gain switching, we can use the following differential equations for the number of carriers N , and the number of photons S . The table below gives the

description and value of the various constants in the two expressions. The following discussion closely follows [13].

$$\frac{dN}{dt} = \frac{I(t)}{eV} - \frac{N}{\tau_s} - \alpha(N - N_0)S \quad (2.1)$$

$$\frac{dS}{dt} = \alpha(N - N_0)S - \frac{S}{\tau_{ph}} + \beta \frac{N}{\tau_s} \quad (2.2)$$

	Description	Value
V	Volume of Interest	$4.2 * 10^{-10} cm^{-3}$
α	Constant	$1.1125 * 10^{-6} cm^3 s^{-1}$
β	Fraction of useful photons from spontaneous emission	10^{-3}
N_0	No. of carriers over which there will be simulated emission instead of absorption	$1.1 * 10^{18} cm^{-3}$
τ_s	Recombination of carrieres by spontaneous emission	4 ns
τ_{ph}	Optical losses in the cavity	2 ps

We provide a Gaussian current pulse with FWHM of 235ps along with a constant biasing current which is 0.75 times the threshold current(26mA). $I(t) = I_b + I_p$. We plot the current, number of carriers and number of photons for varying peak pulse currents and obtain the FWHM of the optical pulses produced. The results of these calculations are very interesting. The current pulse has a FWHM of 235ps long. When the current pulse has a peak amplitude $5I_{th}$, the optical pulse has a FWHM of 200ps. However, if we increase the peak amplitude to $7I_{th}$, the optical pulse has a duration of only 25ps which is shorter than the input current pulse. If we increase the peak current further to $14I_{th}$, the pulse duration decreases further to 15ps. We also see a smaller secondary optical pulse, because the number of carriers rises above the threshold a second time due to the high amplitude of the pulse current.

2.4 Optical pulses from a laser diode

We use the electrical pulses generated from the transistor 2N5192 to drive a semiconductor diode laser. The diode was connected in series with a 66Ω resistor. The diode laser is a simple red diode laser with wavelength of 650nm. The peak optical power obtained was 5mW with a repetition rate of 1.5kHz which was determined by the avalanche pulse generator. The optical pulse was measured using a photodiode and an oscilloscope. The FWHM duration of the pulse is around 7ns as shown in the Figure 2.5 which is similar to the driving current pulse.

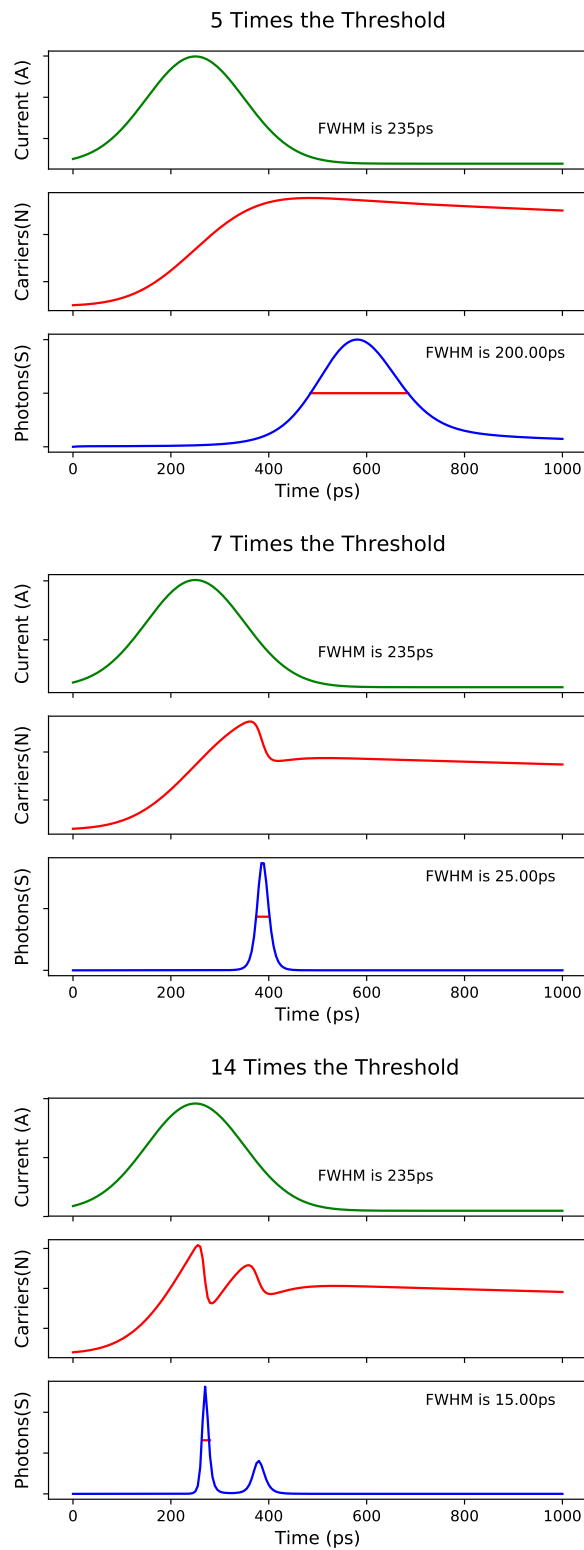


FIGURE 2.4: Current, number of carriers and number of photons as a function of time.

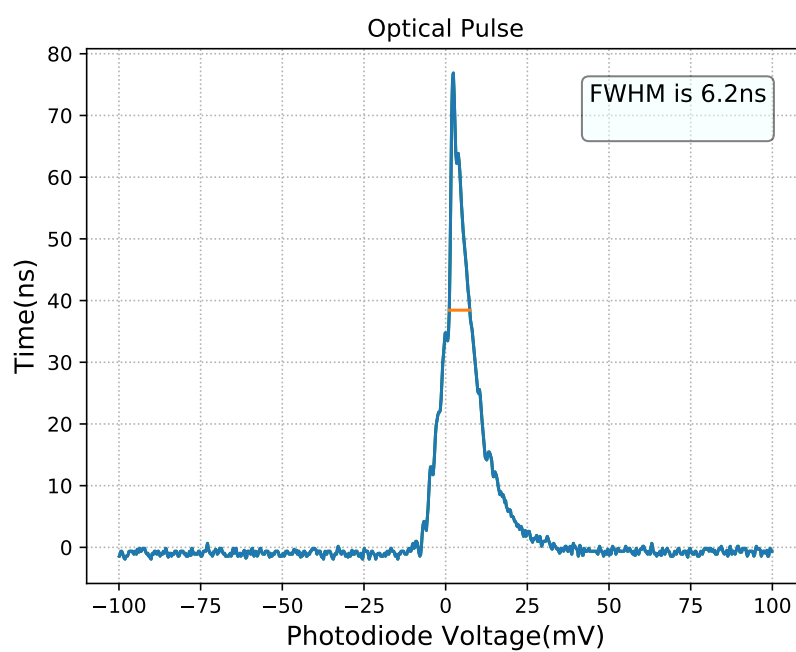


FIGURE 2.5: Optical pulses as measured using a photodiode and oscilloscope.

Appendix A

Finding the spot size in continuous case in a laser cavity

The design of Ti:Sapphire oscillator given in [14] is taken as the reference, which is depicted in Figure A.1. Now, we can find the configurations in which this oscillator will be stable. This is done by using ABCD matrices for Gaussian beams. An introduction to ABCD matrices and Gaussian beams can be found in [15]. The ABCD matrices for different components are given in Table A.1. The following discussion closely follows [16].

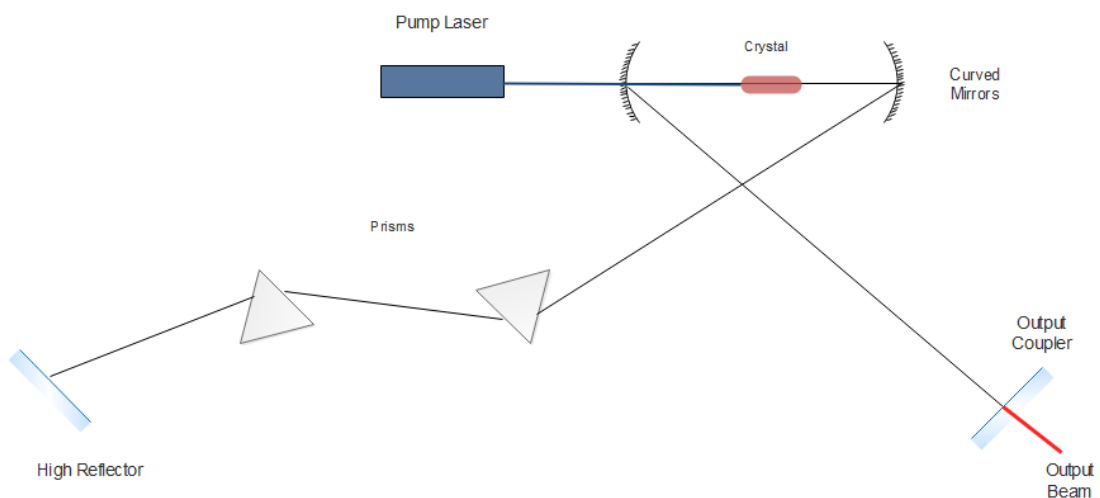


FIGURE A.1: Schematic diagram for the X-folded Ti:Sapphire laser cavity with two arms.

The length of the two arms and the focal length of the focusing mirrors are kept constant. Only the distance between the two curved mirrors is a variable. This is quantified by the cavity parameter δ which is defined as the deviation of the two focusing mirrors from a perfect telescope. In the perfect telescope limit, both the beams are collimated in the both the arms. This implies that δ is equal to the optical path length between the two curved mirrors minus 2 times focal Length of the curved mirrors.

First, We have to write the ABCD matrix for the round trip of the oscillator. As we know, to find the round trip matrix, we just have to multiply the ABCD matrices of the individual components in order. We don't need to write the ABCD matrices for the prisms because their dispersion effect cannot be modeled by the ABCD matrices, and since the prisms do not change the path of the beam away from the principle axis their ABCD matrix is the unit matrix. The ABCD matrices for different components are given in the following table,

Component	Abbreviation	ABCD Matrix
Short Arm	SA	$\begin{bmatrix} 1 & 59 \\ 0 & 1 \end{bmatrix}$
Focussing Mirrors	M	$\begin{bmatrix} 1 & 0 \\ -2/10 & 1 \end{bmatrix}$
Crystal	Cry	$\begin{bmatrix} 1 & 1.76 * 0.475 \\ 0 & 1 \end{bmatrix}$
Long Arm	LA	$\begin{bmatrix} 1 & 101 \\ 0 & 1 \end{bmatrix}$
Crystal to Focussing Mirrors	CM	$\begin{bmatrix} 1 & 4.164 + \delta/2 \\ 0 & 1 \end{bmatrix}$

TABLE A.1: ABCD matrices for various components of the oscillator

We start at the end mirror of the short arm. The round trip matrix can be written as

$$RTM = SA * M * CM * Cry * CM * M * LA * LA * M * CM * Cry * CM * M * SA$$

We know that the q-parameter of the Gaussian beam after passing through an optical component with ABCD matrix will be given by

$$q_2 = \frac{Aq_1 + B}{Cq_1 + D} \quad (\text{A.1})$$

For the oscillator to be stable, the beam after making a round trip must be the same as the original beam. We start by taking the q-parameter at one of the end mirrors and then propagate the beam by the round trip matrix of the oscillator. This can be written as the equation,

$$q = \frac{Aq + B}{Cq + D} \quad (\text{A.2})$$

where the ABCD matrix is the round trip ABCD matrix. We can invert this to obtain

$$\frac{1}{q} = \frac{C + D/q}{A + B/q} \quad (\text{A.3})$$

This is a simple quadratic equation, solving for $1/q$, we obtain

$$\frac{1}{q} = \frac{D - A}{2B} - \frac{i\sqrt{1 - (A + D)^2/4}}{|B|} \quad (\text{A.4})$$

From the inverse q-parameter, we can find the spot size of the beam at one of the end mirrors which is given by,

$$\omega^2 = \frac{|B|\lambda}{\pi} \sqrt{\frac{1}{1 - (A + D)^2/4}} \quad (\text{A.5})$$

This is done by equating the imaginary part of the $1/q$ with the standard expression for $1/q$ which is,

$$\frac{1}{q(z)} = \frac{1}{R(z)} - \frac{i\lambda_0}{\pi n\omega(z)^2} \quad (\text{A.6})$$

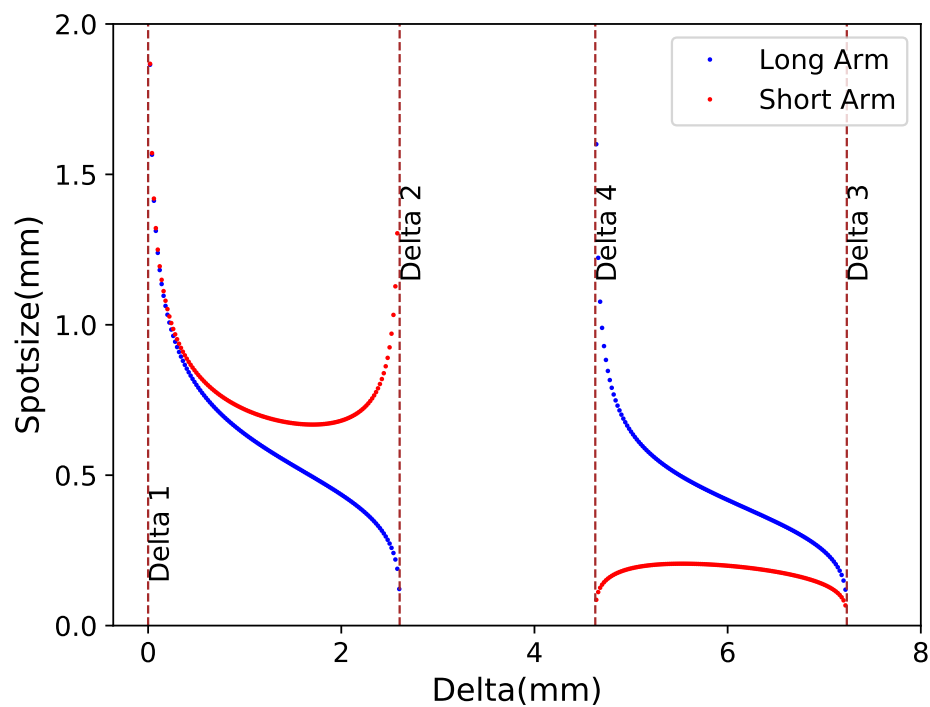
Now we can plot the spot size of the Gaussian beam as a function of the separation between the curved mirrors (The parameter δ). As is easily seen from the expression for the spot size, the cavity is stable only when $-2 < (A + D) < 2$. This gives a range for δ for which the cavity will be stable, as seen in the plot of the spot size at the short arm end mirror.

As shown above, we can use ABCD matrices to find the spot sizes in continuous mode but Kerr Lens produces non-linearity in the cavity which cannot be modeled by ABCD matrices.

```

1 import matplotlib.pyplot as plt
2 import numpy as np
3 from sympy import Symbol, solve
4 from matplotlib.ticker import StrMethodFormatter

```

FIGURE A.2: Spot size as a function of the cavity parameter δ

```

5
6 wl = 800E-6 #Define wavelength
7
8 #define a function to translate inverse q paramater by ABCD
  element RTM
9 def translation(RTM, iq):
10     A = RTM[0,0]
11     B = RTM[0,1]
12     C = RTM[1,0]
13     D = RTM[1,1]
14     return (C+D*iq)/(A+B*iq)
15
16 #find the eigenvalue inverse q-parameter given a round trip matrix
  RTM
17 def eigenq(RTM):
18     A = RTM[0,0]
19     B = RTM[0,1]
20     C = RTM[1,0]

```

```

21     D = RTM[1,1]
22     return (D-A)/(2*B) - 1j*np.sqrt(1-((A+D)**2)/4) / abs(B)
23
24 #find the spotsize given inverse q parameter
25 def spotsize(iq):
26     X=iq.imag
27     return np.sqrt(-wl/(np.pi*X))
28
29 #Cavity elements that are static
30 short_arm      = np.matrix([[1.,590.],[0.,1]])
31 long_arm       = np.matrix([[1.,1010.],[0.,1]])
32 cw_crystal     = np.matrix([[1.,1.76*5],[0.,1]])
33 curved_mirror  = np.matrix([[1.,0.],[-1/50,1]])
34
35 #def the RTM as a function of the distance b/w the crystal and the
    curved mirror
36 def cavity(x):
37     mtoc = np.matrix([[1.,x],[0.,1.]]) #Short Arm
38     ctom = mtoc #Long Arm
39     return short_arm*curved_mirror*mtoc*cw_crystal*ctom*
    curved_mirror*long_arm*long_arm*curved_mirror*ctom*cw_crystal*
    mtoc*curved_mirror*short_arm
40
41 #Symbolically solve the continuous case and find the limits
42 fx = Symbol("fx")
43 z=fx
44 llimit = solve(cavity(z)[0,0]+cavity(z)[1,1] - 2)
45 ulimit = solve(cavity(z)[0,0]+cavity(z)[1,1] + 2)
46
47
48 dist=[]
49 ss=[]
50 sslong = []
51
52 for i in range(0,5000):
53     x = i/100
54     RTM = cavity(x)

```

```
55     ctom = np.matrix([[1 , x] , [0 , 1]])
56     mtoc = ctom
57     if abs(RTM[0,0]+RTM[1 , 1])<2 and RTM[0 , 1]!=0: #Condition for
stable cavity
58         iq = eigenq(RTM)
59         iqlong = translation(long_arm*curved_mirror*ctom*
cw_crystal*mtoc*curved_mirror*short_arm , iq) #find
the inverse q parameter on the long arm end mirror
60
61         dist.append(2*x-91.2) #convert the distance b/w crystal
and mirror to delta
62         ss.append(spotsize(iq))
63         sslong.append(spotsize(iqlong))
64
65     fig = plt.figure()
66     ax = fig.add_subplot(111)
67
68     plt.plot(dist , sslong , 'bo' , markersize = '1' , label="Long Arm")
69     plt.plot(dist , ss , 'ro' , markersize = '1' , label="Short Arm")
70     plt.xlabel(" Delta (mm)" , fontsize=14)
71     plt.ylabel(" Spotsize (mm)" , fontsize=14)
72     plt.ylim(0,2)
73
74     #Convert the Stability limit values to appropriate delta values
75
76     llimit = [2*x-91.2 for x in llimit]
77     ulimit = [2*x-91.2 for x in ulimit]
78
79     #Plot the stability limit lines corresponding to different Delta
values
80     plt.axvline(llimit[0] , linestyle='dashed' , linewidth='1' , color='
brown')
81     plt.text(llimit[0] , 0.4 , 'Delta 1' , rotation=90 , fontsize=12)
82
83     plt.axvline(ulimit[0] , linestyle='dashed' , linewidth='1' , color='
brown')
84     plt.text(ulimit[0] , 1.4 , 'Delta 2' , rotation=90 , fontsize=12)
```

```
85
86 plt.axvline(llimit[1], linestyle='dashed', linewidth='1', color='
    brown')
87 plt.text(llimit[1], 1.4, 'Delta 3', rotation=90, fontsize=12)
88
89 plt.axvline(ulimit[1], linestyle='dashed', linewidth='1', color='
    brown')
90 plt.text(ulimit[1], 1.4, 'Delta 4', rotation=90, fontsize=12)
91
92
93 #Formatting the ticks
94 plt.gca().yaxis.set_major_formatter(StrMethodFormatter('{x:,.1f}'))
95
96 plt.yticks(np.arange(0, 2.5, step=0.5), fontsize=12)
97 plt.xticks(np.arange(0, 10, step=2), fontsize=12)
98
99 plt.legend(fontsize=12)
100
101 #To get the plot in a full sized window. For formatting
102 #manager = plt.get_current_fig_manager()
103 #manager.resize(*manager.window.maxsize())
104
105 #Show and save the figure
106 plt.show()
107 fig.savefig('01_yefet.pdf', format='pdf', dpi=1200)
```


Appendix B

Beam shaping simulations

B.1 Before collimation

```
1 import numpy as np
2 import matplotlib.pyplot as plt
3
4 def spotsizes(iq):
5     #find the spot size given the inverse q parameter in cm
6     X=iq.imag
7     return np.sqrt(-wl/(np.pi*X))
8
9 def translation(iq,RTM):
10    #finds the inverse q parameter after passing through elements
    RTM
11    A = RTM[0,0]
12    B = RTM[0,1]
13    C = RTM[1,0]
14    D = RTM[1,1]
15    return (C+D*iq)/(A+B*iq)
16
17 lens1_f = 500
18 lens2_f = -50
19 pos_start = -200
20 pos_lens1 = 0
```

```
21 pos_lens2 = 530
22 pos_end   = 560
23
24 lens1 = np.matrix([[1.,0.],[-1/lens1_f,1]])
25
26 #-----Fast Axis
27 M2 = 1.5
28 wl = M2*470E-6
29 beam_r = 0.44
30
31 ss=[]
32 distance=[]
33 # from start to end
34
35 iq = 0 - wl*1j/(np.pi*beam_r*beam_r)
36
37 for i in range(pos_start, pos_end):
38     ss.append(spotsize(iq))
39     distance.append(i)
40     iq=translation( iq , np.matrix( [[1,1],[0,1]] ) )
41 negs = [-x for x in ss]
42 negdis = [-x for x in distance]
43
44 fig = plt.figure()
45 ax = fig.add_subplot(111)
46
47 plt.plot(negdis, negs, color="darksalmon", label='Fast Axis')
48 plt.plot(negdis, ss, color="darksalmon")
49
50
51
52 #-----SLOW-AXIS
53 M2 = 12
54 wl = M2*470E-6
55 beam_r = 2.2
```



```
56
57 lens2 = np.matrix([[1.,0.],[-1/49.57,1]])
58
59 iq = 0 - wl*1j/(np.pi*beam_r*beam_r)
60
61 ss=[]
62 distance=[]
63 # from start to Lens1
64
65 for i in range(pos_start , pos_lens1):
66
67     ss.append(spotsize(iq))
68     distance.append(i)
69     iq=translation( iq , np.matrix( [[1,1],[0,1]] ) )
70
71 #from lens1 to lens2
72 iq = translation(iq , lens1)
73 for i in range(pos_lens1 , pos_lens2):
74     ss.append(spotsize(iq))
75     distance.append(i)
76     iq=translation( iq , np.matrix( [[1,1],[0,1]] ) )
77
78 #from lens1 to lens2
79 iq = translation(iq , lens2)
80 for i in range(pos_lens2 , pos_end):
81     ss.append(spotsize(iq))
82     distance.append(i)
83     iq=translation( iq , np.matrix( [[1,1],[0,1]] ) )
84
85 negs = [-x for x in ss]
86 negdis = [-x for x in distance]
87
88
89
90 plt.plot(negdis , negs , color="cornflowerblue" , label='Slow Axis')
91 plt.plot(negdis , ss , color="cornflowerblue")
92
```

```
93 plt.axvline(-pos_lens1, linestyle='dashed', linewidth='1', color='
    red')
94 plt.text(-pos_lens1+2, -1.5, 'Cylindrical\n500mm', rotation=90)
95
96 plt.axvline(-pos_lens2, linestyle='dashed', linewidth='1', color='
    red')
97 plt.text(-pos_lens2+2, -1.5, 'Cylindrical\n50mm', rotation=90)
98
99 plt.axvline(-pos_start, linestyle='dashed', linewidth='1', color='
    red')
100 plt.text(-pos_start+2, -0.5, 'To Focusing Optics', rotation=90)
101
102 plt.axvline(-pos_end, linestyle='dashed', linewidth='1', color='red'
    )
103 plt.text(-pos_end+2, -0.5, 'Aspheric', rotation=90)
104
105
106
107 plt.xlabel('Distance (mm)', fontsize=12)
108 plt.ylabel('Spotsize (mm)', fontsize=12)
109 #plt.xlim(83, 90)
110 #plt.ylim(-0.120, .120)
111 plt.legend()
112 plt.show()
113
114 fig.savefig('Before_collimation.pdf', format='pdf', dpi=1200)
```

B.2 After collimation

```

1 import numpy as np
2 import matplotlib.pyplot as plt
3
4 def spotsize(iq):
5     #find the spot size given the inverse q paramter in cm
6     X=iq.imag
7     return np.sqrt(-wl/(np.pi*X))
8
9 def translation(iq,RTM):
10    #finds the inverse q parameter after passing through elements
    RTM
11    A = RTM[0,0]
12    B = RTM[0,1]
13    C = RTM[1,0]
14    D = RTM[1,1]
15    return (C+D*iq)/(A+B*iq)
16
17 lens1_f = 105
18 lens2_f = 50
19 pos_start = -50
20 pos_lens1 = 0
21 pos_lens2 = 61
22 pos_end = 110
23
24 lens1 = np.matrix([[1.,0.],[-1/lens1_f,1]])
25
26 #-----FAST-AXIS-----
27 M2 = 1.5
28 wl = M2*470E-6
29 beam_r = 0.44
30
31 lens2 = np.matrix([[1.,0.],[-1/50.42,1]])
32
33 iq = 0 - wl*1j/(np.pi*beam_r*beam_r)

```

```
34
35 distance=[]
36 # from start to Lens1
37
38 ss=[]
39 for i in range(pos_start*10,pos_lens1*10):
40     ss.append(spotsize(iq))
41     distance.append(i/10)
42     iq=translation( iq , np.matrix( [[1,0.1],[0,1]] ) )
43
44 #from lens1 to lens2
45 iq = translation(iq, lens1)
46 for i in range(pos_lens1*10,pos_lens2*10):
47     ss.append(spotsize(iq))
48     distance.append(i/10)
49     iq=translation( iq , np.matrix( [[1,0.1],[0,1]] ) )
50
51 #from lens1 to lens2
52 iq = translation(iq, lens2)
53 for i in range(pos_lens2*10,pos_end*10):
54     ss.append(spotsize(iq))
55     distance.append(i/10)
56     iq=translation( iq , np.matrix( [[1,0.1],[0,1]] ) )
57
58 print("Fast Axis")
59 print("Diameter", min(ss)*2000,"um")
60 print(distance[ss.index(min(ss))])
61
62 negs = [-x for x in ss]
63
64 fig = plt.figure()
65 ax = fig.add_subplot(111)
66
67 plt.plot(distance, negs, color="darksalmon", label='Fast Axis')
68 plt.plot(distance, ss, color="darksalmon")
69
```

```

70 #-----SLOW-AXIS
71 M2 = 12
72 wl = M2*470E-6
73 beam_r = 2.2
74
75 lens2 = np.matrix([[1.,0.],[-1/49.57,1]])
76
77 iq = 0 - wl*1j/(np.pi*beam_r*beam_r)
78
79 ss=[]
80 distance=[]
81 # from start to Lens1
82
83 for i in range(pos_start*10,pos_lens1*10):
84     ss.append(spotsize(iq))
85     distance.append(i/10)
86     iq=translation( iq , np.matrix( [[1,0.1],[0,1]] ) )
87
88 #from lens1 to lens2
89 iq = translation(iq,lens1)
90 for i in range(pos_lens1*10,pos_lens2*10):
91     ss.append(spotsize(iq))
92     distance.append(i/10)
93     iq=translation( iq , np.matrix( [[1,0.1],[0,1]] ) )
94
95 #from lens1 to lens2
96 iq = translation(iq,lens2)
97 for i in range(pos_lens2*10,pos_end*10):
98     ss.append(spotsize(iq))
99     distance.append(i/10)
100    iq=translation( iq , np.matrix( [[1,0.1],[0,1]] ) )
101
102 print("Slow Axis")
103 print("Diameter",min(ss)*2000,"um")
104 print(distance[ss.index(min(ss))])
105

```

```
106 negs = [-x for x in ss]
107 plt.plot(distance, negs, color="cornflowerblue", label='Slow Axis')
108 plt.plot(distance, ss, color="cornflowerblue")
109
110 plt.axvline(pos_lens1, linestyle='dashed', linewidth='1', color='red
    ')
111 plt.text(pos_lens1, -0.5, '105mm Lens', rotation=90)
112
113 plt.axvline(pos_lens2, linestyle='dashed', linewidth='1', color='red
    ')
114 plt.text(pos_lens2, -0.5, '100mm ROC', rotation=90)
115
116 plt.xlabel('Distance (mm)', fontsize=13)
117 plt.ylabel('Spotsize (mm)', fontsize=13)
118 #plt.xlim(80, 89)
119 #plt.ylim(-0.120, .120)
120 plt.legend()
121 plt.show()
122
123 fig.savefig('focusing.pdf', dpi=1200)
```

Appendix C

Gain switching using RK4

```
1 #Picosecond Laser
2 #Gain Switching
3 #Runge Kutta Method 4
4
5 import numpy as np
6 import matplotlib.pyplot as plt
7
8
9 ec = 1.602E-19          #Electronic Charge
10 volume = 4.2E-10      #volume of the active region
11 beta = 1E-3           #constant to determine how many
                        #spontaneous give meaningful stimulated radn
12 alpha = 1.1125E-6     #constant
13 N0 = 1.1E18           #determines optical gain or loss
14 taus = 4E-9           #Spontaneous recombination of carriers
                        #lifetime
15 tauph = 2E-12         #losses due to cavity photon lifetime
16
17 #Current Pulse Gaussian 100ps
18 def currentpulse(x):
19     return 0.75*0.026 + 14*0.026*np.exp(-0.5*( (x-250E-12)/100E-12
20         )**2 )
21
22 pstime = np.arange(0,1E-9,5E-12)
```

```
22 current = [currentpulse(x) for x in pstime]
23
24 def dNdt(t,N,S):
25     return currentpulse(t)/(ec*volume) - N/taus - alpha*(N - N0)*S
26
27 def dSdt(t,N,S):
28     return alpha*(N - N0)*S - S/tauph + beta*N/taus
29
30 Nlist = []
31 Slist = []
32
33 Ni = 1.1E18
34 Si = 0
35 h = 5E-12
36
37 for i in pstime:
38     ti = i
39     Nlist.append(Ni)
40     Slist.append(Si)
41
42     k0 = h*dNdt(ti ,Ni ,Si)
43     l0 = h*dSdt(ti ,Ni ,Si)
44
45     k1 = h*dNdt(ti + 0.5*h, Ni + 0.5*k0 ,Si + 0.5*l0)
46     l1 = h*dSdt(ti + 0.5*h, Ni + 0.5*k0 ,Si + 0.5*l0)
47
48     k2 = h*dNdt(ti + 0.5*h, Ni + 0.5*k1 ,Si + 0.5*l1)
49     l2 = h*dSdt(ti + 0.5*h, Ni + 0.5*k1 ,Si + 0.5*l1)
50
51     k3 = h*dNdt(ti + h, Ni + k2 ,Si + l2)
52     l3 = h*dSdt(ti + h, Ni + k2 ,Si + l2)
53
54     Ni = Ni + 1/6*(k0 + 2*k1 + 2*k2 + k3)
55     Si = Si + 1/6*(l0 + 2*l1 + 2*l2 + l3)
56
57
58 X=pstime
```



```

59 Y=Slist
60 def takeClosest(num, collection):
61     return min(collection, key=lambda x: abs(x-num))
62 maxind = Y.index(max(Y))
63 FWHM1 = takeClosest( max(Y)/2, Y[:maxind] )
64 FWHM2 = takeClosest( max(Y)/2, Y[maxind:] )
65
66 LX = [X[Y.index(FWHM1)], X[Y.index(FWHM2)]]
67 LY = [max(Y)/2, max(Y)/2]
68 LX = [x*1E12 for x in LX]
69 FWHM= LX[1]-LX[0]
70 print(FWHM, LX, LY)
71
72
73
74 fig, (ax1, ax2, ax3) = plt.subplots(3, 1, sharex=True)
75 ax1.plot(pstime*1E12, current, color='g')
76 ax2.plot(pstime*1E12, Nlist, color='red')
77 ax3.plot(LX, LY, 'r')
78 ax3.plot(pstime*1E12, Slist, color='b')
79
80 plt.text(0.3, 1.2, "14 Times the Threshold", fontsize=14, transform=
    ax1.transAxes)
81 plt.text(0.5, 0.3, "FWHM is 235ps", transform=ax1.transAxes)
82 plt.text(0.7, 0.8, "FWHM is {0:.2f}ps".format(FWHM), transform=ax3.
    transAxes)
83
84 ax1.set_ylabel('Current (A)', fontsize=12)
85 ax2.set_ylabel('Carriers (N)', fontsize=12)
86 ax3.set_ylabel('Photons (S)', fontsize=12)
87 ax3.set_xlabel('Time (ps)', fontsize=12)
88 ax1.set_yticklabels([], [])
89 ax2.set_yticklabels([], [])
90 ax3.set_yticklabels([], [])
91 plt.show()
92 fig.savefig('14lth.pdf', format='pdf', dpi=1200)

```


Bibliography

- [1] Jim Williams. High speed amplifier techniques. pages 93–95, Aug 1991. URL <https://www.analog.com/media/en/technical-documentation/application-notes/an47fa.pdf>.
- [2] K. Gürel, V. J. Wittwer, M. Hoffmann, C. J. Saraceno, S. Hakobyan, B. Resan, A. Rohrbacher, K. Weingarten, S. Schilt, and T. Südmeyer. Green-diode-pumped femtosecond ti:sapphire laser with up to 450 mw average power. *Opt. Express*, 23(23):30043–30048, Nov 2015. doi: 10.1364/OE.23.030043. URL <http://www.opticsexpress.org/abstract.cfm?URI=oe-23-23-30043>.
- [3] S Nakamura. Current status and future prospects of ingan-based laser diodes. Jan 2010. URL https://www.jsap.or.jp/jsapi/Pdf/Number01/Vol-1_Cutting%20Edge.pdf.
- [4] Peter W. Roth, Alexander J. Maclean, David Burns, and Alan J. Kemp. Directly diode-laser-pumped ti:sapphire laser. *Opt. Lett.*, 34(21):3334–3336, Nov 2009. doi: 10.1364/OL.34.003334. URL <http://ol.osa.org/abstract.cfm?URI=ol-34-21-3334>.
- [5] Khaled Gasmi Taofeek O. Adigun Watheq Al-Basheer, Abdulaziz Aljalal. High-resolution investigation of longitudinal modes of a gan-based blue laser diode. 10231, 2017. doi: 10.1117/12.2264383. URL <https://doi.org/10.1117/12.2264383>.
- [6] Sterling Backus, Matt Kirchner, Charles Durfee, Margaret Murnane, and Henry Kapteyn. Direct diode-pumped kerr lens 13 fs ti:sapphire ultrafast oscillator using a single blue laser diode. *Opt. Express*, 25(11):12469–12477, May 2017. doi: 10.1364/OE.25.012469. URL <http://www.opticsexpress.org/abstract.cfm?URI=oe-25-11-12469>.
- [7] Peter W. Roth, Alexander J. Maclean, David Burns, and Alan J. Kemp. Direct diode-laser pumping of a mode-locked ti:sapphire laser. *Opt. Lett.*, 36(2):304–306, Jan 2011. doi: 10.1364/OL.36.000304. URL <http://ol.osa.org/abstract.cfm?URI=ol-36-2-304>.

- [8] Charles G. Durfee, Tristan Storz, Jonathan Garlick, Steven Hill, Jeff A. Squier, Matthew Kirchner, Greg Taft, Kevin Shea, Henry Kapteyn, Margaret Murnane, and Sterling Backus. Direct diode-pumped kerr-lens mode-locked ti:sapphire laser. *Opt. Express*, 20(13):13677–13683, Jun 2012. doi: 10.1364/OE.20.013677. URL <http://www.opticsexpress.org/abstract.cfm?URI=oe-20-13-13677>.
- [9] R. Sawada, H. Tanaka, R. Kariyama, K. Hirosawa, and F. Kannari. Demonstration of femtosecond ti:sapphire laser oscillation pumped by ingan diode lasers. In *2015 11th Conference on Lasers and Electro-Optics Pacific Rim (CLEO-PR)*, volume 2, pages 1–2, Aug 2015. doi: 10.1109/CLEOPR.2015.7375939.
- [10] Sterling Backus, Matt Kirchner, Randy Lemons, David Schmidt, Charles Durfee, Margaret Murnane, and Henry Kapteyn. Direct diode pumped ti:sapphire ultrafast regenerative amplifier system. *Opt. Express*, 25(4):3666–3674, Feb 2017. doi: 10.1364/OE.25.003666. URL <http://www.opticsexpress.org/abstract.cfm?URI=oe-25-4-3666>.
- [11] Orazio Svelto. *Transient Laser Behavior*, pages 313–373. Springer US, Boston, MA, 2010. ISBN 978-1-4419-1302-9. doi: 10.1007/978-1-4419-1302-9_8. URL https://doi.org/10.1007/978-1-4419-1302-9_8.
- [12] Ari Kilpel and Juha Kostamovaara. Laser pulser for a time-of-flight laser radar. *Review of Scientific Instruments*, 68(6):2253–2258, 1997. doi: 10.1063/1.1148133. URL <https://doi.org/10.1063/1.1148133>.
- [13] P. Paulus, R. Langenhorst, and D. Jager. Generation and optimum control of picosecond optical pulses from gain-switched semiconductor lasers. *IEEE Journal of Quantum Electronics*, 24(8):1519–1523, Aug 1988. ISSN 0018-9197. doi: 10.1109/3.7078.
- [14] Melanie T. Asaki, Chung-Po Huang, Dennis Garvey, Jianping Zhou, Henry C. Kapteyn, and Margaret M. Murnane. Generation of 11-fs pulses from a self-mode-locked ti:sapphire laser. *Opt. Lett.*, 18(12):977–979, Jun 1993. doi: 10.1364/OL.18.000977. URL <http://ol.osa.org/abstract.cfm?URI=ol-18-12-977>.
- [15] Orazio Svelto. *Ray and Wave Propagation Through Optical Media*, pages 131–161. Springer US, Boston, MA, 2010. ISBN 978-1-4419-1302-9. doi: 10.1007/978-1-4419-1302-9_4. URL https://doi.org/10.1007/978-1-4419-1302-9_4.
- [16] Shai Yefet and Avi Pe’er. A Review of Cavity Design for Kerr Lens Mode-Locked Solid-State Lasers. *arXiv e-prints*, art. arXiv:1501.01158, Jan 2015.